



Thermally activated transformation of the adsorption configurations of a complex molecule on a Cu(1 1 1) surface

X.Q. Shi^a, W.H. Wang^b, S.Y. Wang^b, N. Lin^b, M.A. Van Hove^{a,*}

^a Department of Physics and Materials Science, City University of Hong Kong, Hong Kong, China

^b Department of Physics, The Hong Kong University of Science and Technology, Clear Water Bay, Hong Kong, China

ARTICLE INFO

Article history:

Received 11 January 2011

Received in revised form 28 March 2011

Accepted 30 March 2011

Available online 25 May 2011

Keywords:

Surfaces
Interfaces
Catalysis
STM
DFT

ABSTRACT

Temperature-dependent transformations of the adsorption configuration of a molecule containing 2,2':6',2''-terpyridine (terpy) end-groups on a flat Cu(1 1 1) surface are studied by a combination of scanning tunneling microscopy (STM) experiments and density functional theory (DFT) calculations. Several quite different adsorption configurations are detected for the terpy end-group, including flat physisorption, distorted chemisorption through N–Cu bonds, and H-dissociative chemisorption through N–Cu and C–Cu bonds. These illustrate and explore various bonding modes of molecules at surfaces, which also imply a greater richness of reaction pathways, both of which are of central importance in a wide variety of heterogeneous catalytic processes on metal catalysts. As deposited on the cold substrate (near 77 K), the molecules are preferably chemisorbed on the surface through N–Cu bonds. With increasing annealing temperature, the molecules are converted to a physisorption configuration at and above 300 K, and above 370 K a small fraction of molecules undergoes dehydrogenation and chemisorb on the surface through N–Cu and C–Cu bonds. The present study demonstrates that the combination of STM measurements and DFT calculations is very effective for probing the atomic details of molecular adsorption configurations on surfaces.

© 2011 Elsevier B.V. All rights reserved.

1. Introduction

Probing the molecule–surface interactions is of fundamental importance for understanding heterogeneous catalysis [1,2]. While much has been accomplished in understanding the properties of smaller molecules on well-defined surfaces [3,4], rather little is known about larger molecules on such surfaces. In general, the interactions of molecules with surfaces depend on many factors; large molecules offer more degrees of freedom, as well as mixed modes of adsorption, and therefore are even more affected by various parameters. Particularly important among such factors is the temperature of deposition and/or annealing, since thermal energy can often easily transform the bonding configurations of a molecule on a surface [5].

Here we report investigations on the temperature dependence of different bonding configurations of a complex molecule adsorbed on a Cu(1 1 1) surface. The molecule, *tpy*-(*ph*)₂-*tpy*, contains a biphenyl central group terminated by 2,2':6',2''-terpyridine (*tpy*) functional groups at both ends (Fig. 1). This somewhat complex system serves as a model to investigate molecule–metal interactions for molecules containing multiple chemical groups [6], and

shows interesting temperature-dependent changes in the mode of adsorption. The central biphenyl group is known to physisorb on noble metal (1 1 1) surfaces [7,8]. However, the *tpy* end-group may be either physisorbed, with the *tpy* group lying flat on the surface, or chemisorbed, with the heteroatom N bonding to the metal surface.

In this work, we study the temperature-dependent transformation of these molecular adsorption configurations by combining experimental scanning tunneling microscopy (STM) with density functional theory (DFT) calculations. The major findings are: as deposited on the cold substrate (near 77 K), the molecules are preferably chemisorbed on the surface through Cu–N bonds; with increasing annealing temperature, the molecules are converted to a physisorption configuration at and above 300 K, while above 370 K a small fraction of the molecules undergoes dehydrogenation and chemisorb on the surface through Cu–C and Cu–N bonds. The observed transformations agree with adsorption energies calculated by DFT, which demonstrates that the combination of STM measurements and DFT calculations is very effective for probing the atomic details of complex molecular adsorption on surfaces.

2. Method

The experiments were carried out in an ultrahigh vacuum scanning tunneling microscope system (Omicron) operated at low temperature. A Cu(1 1 1) single crystal was cleaned by cycles of

* Corresponding author. Tel.: +852 3442 7848; fax: +852 3442 0539.

E-mail address: vanhove@cityu.edu.hk (M.A. Van Hove).

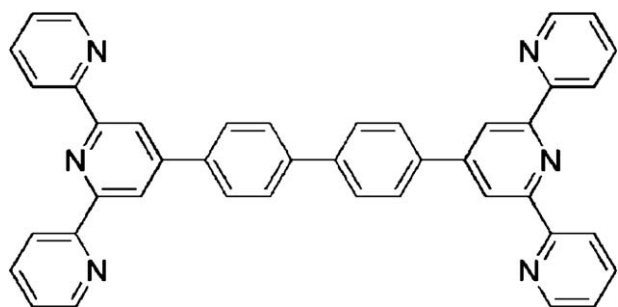


Fig. 1. Structure of a free $tpy-(ph)_2-tpy$ molecule, which is terminated by tpy functional groups at both ends (each tpy group consists of three linked C_5NH_x rings containing one N atom each). This figure shows tpy -ends in their energetically most favorable geometry (trans–trans configuration in terms of N orientation), but the two outer rings of the tpy -end can twist to cis-configurations (by rotation around the C–C bond axes linking C_5NH_x rings).

Ar ion sputtering and annealing. The molecules (in powder form) were evaporated from a molecular beam evaporator (DODECON nanotechnology GmbH) at approximately 600 K and deposited onto the Cu(111) substrate which had been cooled down to 77 K before deposition. After deposition the sample was immediately transferred into the low-temperature STM. The sample was studied by STM at 77 K and 4.9 K. To study the temperature-dependence of the molecular adsorption configuration, the same sample was annealed

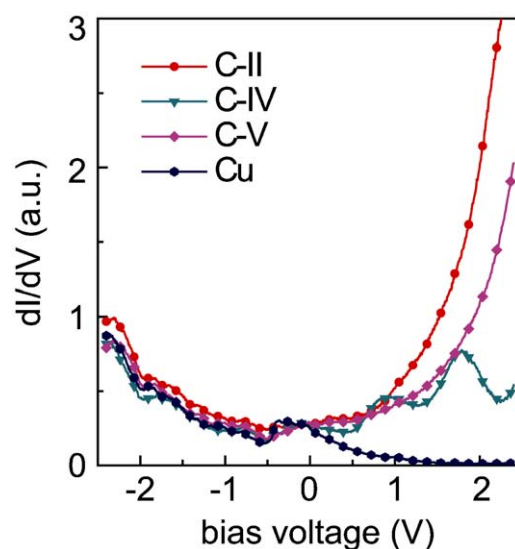


Fig. 3. dI/dV curves measured at the centers of C-II, C-IV and C-V molecules, and in their absence (Cu alone).

to elevated temperatures of 300 K, 373 K, 424 K and 473 K, and large-area STM images were taken at 4.9 K after each annealing process. The STM topographic data were acquired in constant current mode.

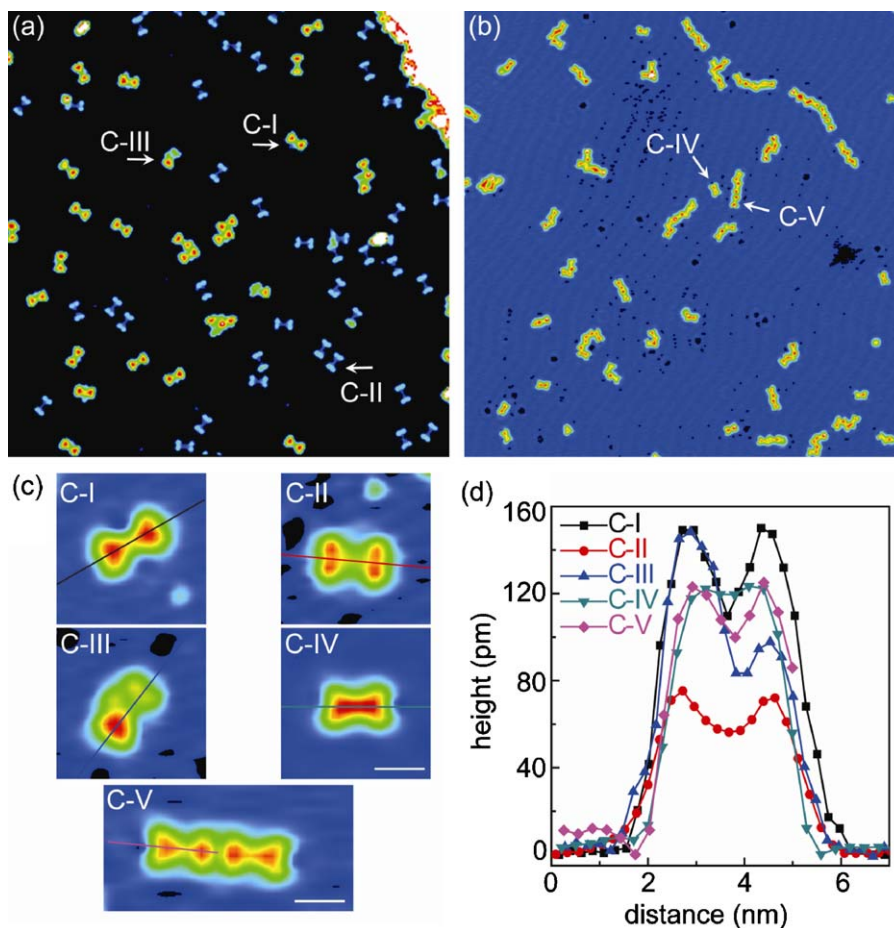


Fig. 2. Five adsorption configurations of $tpy-(ph)_2-tpy$ molecules on Cu(111). (a) STM image of the as-prepared sample (60 nm \times 60 nm). The bright area in the upper right corner is a higher terrace. (b) STM image of the sample annealed at 424 K (100 nm \times 100 nm). Both images were acquired at 4.9 K. The 5 molecular configurations C-I to C-V are marked by arrows. (c) Magnified STM images of the 5 molecular configurations. The common scale bar is 2 nm. (d) Apparent height profiles traced along the molecular long axes of the 5 configurations shown with profile traces in (c). All the images were scanned at -0.2 V and 0.5 nA.

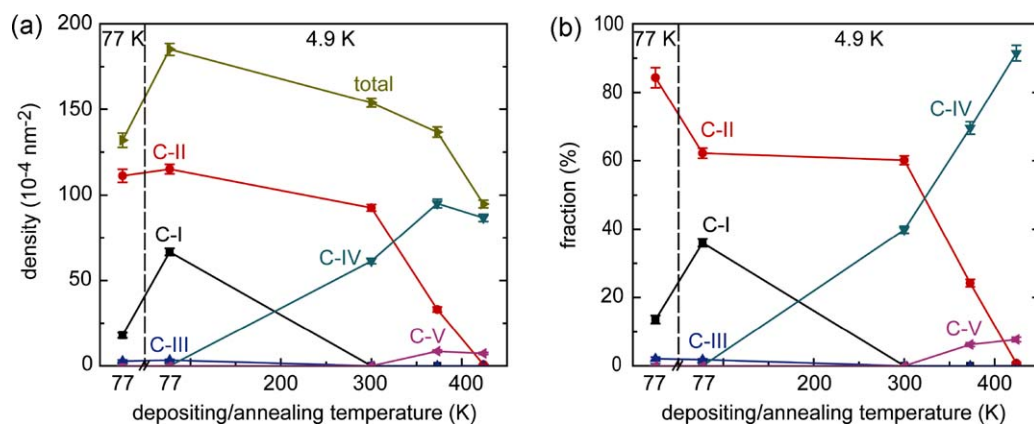


Fig. 4. Densities (a) and fractions (b) of 5 configurations as a function of sample preparation temperature. The data on the left and right of the dashed line were measured at 77 K and 4.9 K, respectively. The error bars in (a) and (b) were given by $\sqrt{(n_i)/S}$ and $\sqrt{(n_i)/N}$, respectively, where n_i is the number of molecules observed in configuration C- i ($i = \text{I, II, III, IV and V}$), S is the total area of the STM images and N is the total number of molecules at a certain sample temperature.

Scanning tunneling spectroscopy (STS) data were acquired by a lock-in technique with a sine modulation of 1517 Hz and 20 mV (rms). To enhance the signal-to-noise ratio at low bias voltage and avoid the molecule being damaged by the high current at high bias voltage, the spectra were acquired in a varied Z mode, in which the tip height Z changes as a function of sample bias voltage V in the measurement ($Z(V) = Z_0 + \Delta Z + \alpha|V|$, in which Z_0 is initial tip height given by a set point, ΔZ is the tip offset and α is the changing parameter). The spectra shown in this paper were measured at -0.2 V and 0.5 nA with $\Delta Z = 0.04 \text{ nm}$ and $\alpha = 0.02 \text{ nm/V}$. Tungsten tips were used in our measurements, which had been subjected to careful cleaning treatments. The features in the spectra are reproducible and independent of the tip electronic structure. The spectra shown in this paper are the averages of 3–6 curves.

The DFT calculation method is the same as in our previous work for the isolated *tpy* molecule adsorbed on Cu(111) [for details see the main text and the Supporting Information of Ref. [6]]. In brief, using the plane-wave-based and projector-augmented-wave [9,10] methods [11,12], including Van der Waals interactions [13,14], for total energies, we study the various adsorption geometries of a single *tpy* molecule on a Cu(111) surface. The simulation models contain a *tpy* molecule (and a *tpy* with missing H) on the surface in a Cu(111)-(6 × 6) supercell with four Cu layers included, of which the bottom two layers are fixed during the structural relaxations.

3. Results

We found that most molecules can be categorized as having one of five distinctive molecular adsorption configurations. Fig. 2(a) and (b) shows two representative STM images of the as-prepared sample and the sample annealed at 424 K, respectively. Both images were acquired at 4.9 K. The five molecular configurations are denoted by C-I to C-V and marked in Fig. 2(a) and (b); they are also shown in Fig. 2(c) in higher resolution. The different characteristics of the five configurations are clearly visible in

the apparent height profiles across the long axis of the molecule as shown in Fig. 2(d). The central biphenyl group of the C-I molecules has an apparent height of 110 pm and the two *tpy* end groups are 40 pm higher than the central biphenyl group. The central biphenyl group of the C-II molecules has an apparent height of ~55 pm with two higher *tpy* end groups at 75 pm. C-III molecules are a combination of C-I and C-II: one *tpy* end group shows the same height as C-I while the other is intermediate between C-I and C-II (~100 pm). C-IV molecules are flatter with a 120 pm central biphenyl group and two 123 pm *tpy* end groups. The central biphenyl group of the C-V molecule pair has an apparent height of 100 pm and its two *tpy* end groups are ~25 pm higher.

In addition, we have used STS to study different molecular configurations. As shown in Fig. 3, in the measurement range of -2.4 V to $+2.4 \text{ V}$, two peaks at 0.90 V and 1.79 V are detected in the dI/dV curve acquired at the center of C-IV molecules, which is in agreement with our previous work [15]. These features indicate that the molecules are weakly coupled to the Cu substrate. In contrast, the dI/dV curves measured at the centers of C-II and C-V molecules are featureless, implying a much more pronounced molecule–substrate coupling.

To investigate the temperature-dependent transformation of these adsorption configurations, we counted the number of molecules of each configuration as the sample temperature was elevated stepwise. For the sample scanned at 77 K, 994 molecules were counted. For the sample scanned at 4.9 K, 2811, 3685, 2068 and 1755 molecules were counted for the depositing/annealing temperature of 77 K, 300 K, 373 K and 424 K, respectively. Fig. 4 shows the density (number of molecules observed in a certain configuration divided by the total area of the STM images) and fraction (number of molecules observed in a certain configuration divided by the total number of molecules) of each configuration as a function of sample preparation temperature. On the as-prepared samples, molecules of the first three types (C-I, II and III) were observed. The density of the C-I molecules which appeared in the

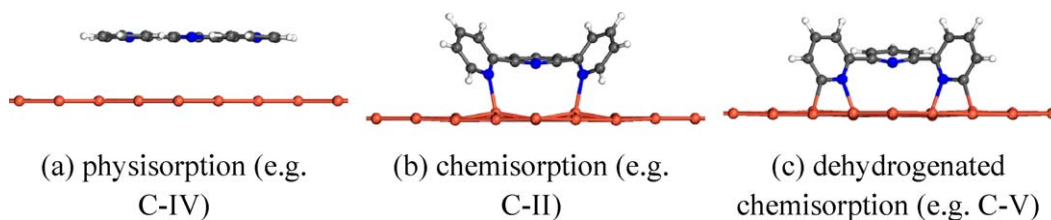


Fig. 5. The three bonding configurations of a single terphenyl (*tpy*) on Cu(111). Only the top Cu layer is shown, exhibiting its distortions. Here and in subsequent figures, Cu is shown red, N blue, C gray and H white. (For interpretation of the references to color in this figure legend, the reader is referred to the web version of the article.)

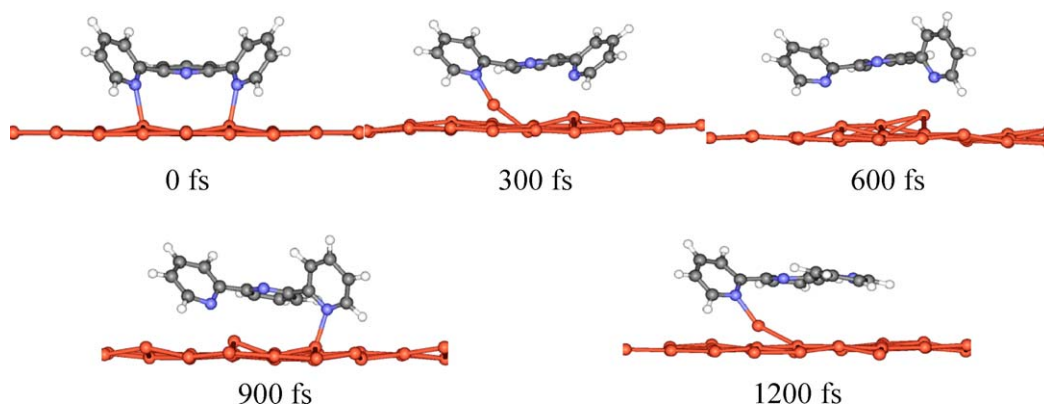


Fig. 6. Snapshots of room temperature molecular dynamics simulations at increasing simulation times (in fs) showing the transformation from chemisorption to physisorption of one *tpy* outer ring. Only the top layer of the Cu substrate is shown.

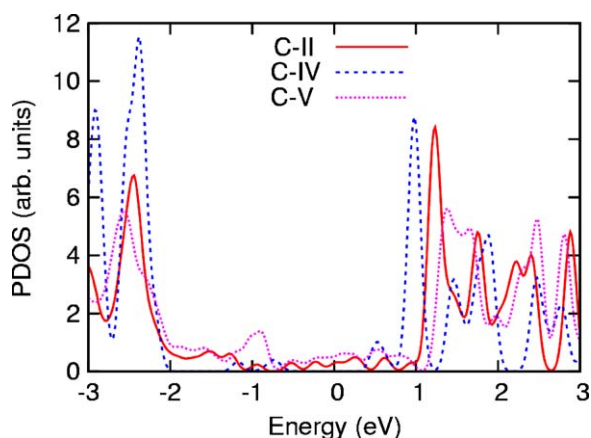


Fig. 7. PDOS of *tpy* in physisorption (C-IV), chemisorption (C-II), and dehydrogenated chemisorption (C-V).

images acquired at 77 K was much lower than that of the same sample acquired at 4.9 K. The lower coverage of C-I at 77 K indicates that the C-I molecules diffuse rapidly at 77 K and thus were not resolved, while they were immobilized at 4.9 K. This observation implies a rather weak molecule–substrate interaction for the C-I configuration. In contrast, the coverages of the C-II or C-III molecules were nearly the same at the two imaging temperatures. So the C-II or C-III molecules have a stronger molecule–substrate interaction than the C-I molecules. The analysis of the images acquired at 4.9 K leads to the conclusion that $62.2 \pm 1.5\%$ of the molecules were of type C-

II, $36.0 \pm 1.1\%$ C-I and the rest C-III. The C-IV molecules were first observed after the sample was annealed to 300 K. At this annealing temperature, the C-I and C-III molecules disappeared and the C-II molecule fraction showed a minor decrease. The number of newly appearing C-IV molecules matches fairly well the reduction of the C-I and C-III molecules. This matching hints that the C-I and C-III molecules were transformed to C-IV at 300 K. After the sample was annealed to 373 K, the number of the C-IV (C-II) molecules further increased (decreased). In the meantime, C-V molecules appeared. It is worth noting that the C-V molecules predominantly appeared in chain-like molecular clusters but rarely as individual molecules. With further annealing of the sample to 424 K, both C-IV and C-V increased whereas the C-II molecules disappeared. After the sample was annealed to 473 K, the molecules assembled into polymers and it became impossible to distinguish individual molecules.

When the sample was annealed to 300 K and even higher temperatures, the total coverage decreased monotonically. This is reasonable because molecules may diffuse to steps and be adsorbed there (these molecules were not counted), or even desorbed from the surface at higher temperature.

4. Theory and discussion

We have explored many possible adsorption configurations of isolated *tpy* molecules adsorbed on the Cu(111) surface using DFT calculations [6]. We found that there are three types of stable or metastable configurations as shown in Fig. 5: (1) physisorption in which the *tpy* group is oriented parallel to the substrate; (2) chemisorption in which the two side pyridine units are tilted down-

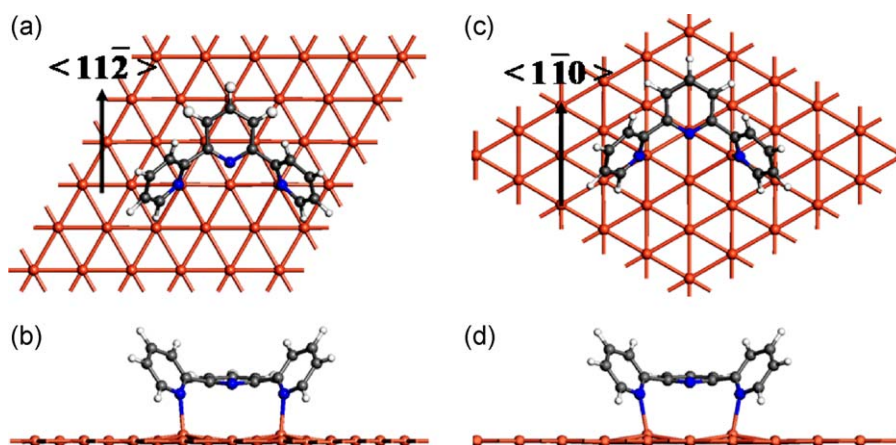


Fig. 8. Two adsorption directions: along the surface $\langle 11\bar{2} \rangle$ and $\langle 1\bar{1}0 \rangle$ directions. (a) and (b) top view and side view for *tpy* along a $\langle 11\bar{2} \rangle$ direction; (c) and (d) top view and side view for *tpy* along a $\langle 1\bar{1}0 \rangle$ direction.

ward, forming Cu–N bonds with the substrate; (3) dehydrogenated chemisorption in which the two side pyridine units are tilted downward as well, with a hydrogen atom dissociated from each side pyridine unit which forms Cu–C bonds.

We assign C-II to the chemisorptions configuration and C-IV to the physisorption configuration based on the following evidence: (1) *ab initio* molecular dynamics simulations, as shown in Fig. 6, reveal that the chemisorption configuration will convert to physisorption at 300 K [6], which explains the conversion of C-II to C-IV at 300 K. (2) STS characteristics reveal that the C-II molecules are strongly coupled to the surface while the C-IV molecules are weakly coupled to the substrate. This is consistent with chemisorption and physisorption, respectively. Fig. 7 shows the projected density of states (PDOS) of *tpy* in physisorption, chemisorption, and dehydrogenated chemisorption. The different broadening in the PDOS for different adsorption modes reflects the increased coupling between the surface and the molecule in chemisorption (and in dehydrogenated chemisorption) compared to physisorption. The C-I molecules are weakly adsorbed and their appearance is intermediate between C-II and C-IV. We thus propose that C-I is an intermediate state between the chemisorption and physisorption configurations, which is formed when the molecules are deposited on a cold substrate. Presumably the C-I molecules are in a metastable configuration in which the molecules are not fully relaxed to the physisorbed configuration. Calculations show that the maximum energy difference is only 0.02 eV during lateral movements of the physisorbed *tpy* across the Cu(1 1 1) surface, which accounts for the fast diffusion of the C-I molecules at 77 K. C-III is a combination of C-I and C-II, containing one *tpy* end group in the intermediate state while the other *tpy* end group is still in the chemisorbed state. Both the C-I and C-III molecules are eventually transformed to the fully relaxed physisorbed configuration C-IV at 300 K, as discussed above.

We assign C-V to dehydrogenated chemisorption. This configuration allows forming strong N–Cu and C–Cu bonds due to the absence of H-surface repulsion. Calculations show that the preferred N–Cu bond length in C-V amounts to 2.01 Å, which is 0.16 Å shorter than the N–Cu bond length in C-II. In C-V the C–Cu bond length is even shorter, 1.98 Å. Thus, both strong Cu–N and strong Cu–C bonds are formed in C-V. On the other hand, dehydrogenation requires overcoming a large reaction barrier and thus may need a higher temperature. Therefore C-V appears at the higher temperatures after overcoming the reaction barrier of dehydrogenation. In addition, the molecules of this configuration cannot be converted to other types because the dehydrogenation is an irreversible reaction.

Finally, we make a rough comparison between the energy barriers from the chemisorbed configuration (C-II) to the physisorbed configuration (C-IV) or to dehydrogenated chemisorption (C-V). The energy barrier from C-II to C-IV is much smaller than that to C-V: the energy barrier in rotating the free molecular outer ring is about 0.63 eV, while the bond dissociation energy of the C–H bond is about 3.4 eV (78 kcal/mol) [16]. The bond dissociation energy of the C–H bond is much higher than the thermal energy in our experiment (the thermal energy at 424 K is 36.5 meV). Interestingly, the C-V molecules were predominantly observed in Cu-coordinated chains, so we propose that the C–H bond dissociation may be catalyzed by individual Cu adatoms on the Cu(1 1 1) surface. To make more specific statements here would benefit from additional experimental structural details of the pairing structure of C-V molecules, in particular concerning the possible locations (and numbers) of Cu adatoms and dissociated H atoms.

5. Comparison of adsorption directions

The above discussion of our theoretical simulations describes the situation when the *terpy* molecule is oriented along the $\langle 1-10 \rangle$ surface directions, as assumed in our previous pure theoretical work [6]. The STM experiments show that the molecules prefer to orient along the $\langle 11-2 \rangle$ surface directions, especially for chemisorption configurations. Therefore, we also calculated the chemisorption geometry for the molecule oriented along the $\langle 11-2 \rangle$ directions (Fig. 8). The results show that both adsorption directions give very similar bond lengths and total energies; and hence the previous discussion carries over without significant change for the experimentally favored orientation. Indeed, for adsorption of the molecule along the $\langle 11-2 \rangle$ surface directions, the differences in the bond lengths and total energy are very small relative to the molecule along the $\langle 1-10 \rangle$ surface directions. The energy is lowered by 0.04 eV and the N–Cu bond length is shortened by 0.01 Å for the *tpy* molecule along the $\langle 11-2 \rangle$ surface directions.

6. Conclusions

We have shown that relatively complex molecules adsorbed on surfaces offer a structural richness that can be fruitfully investigated by means of STM experiments and DFT calculations. For *tpy*-(*ph*)₂-*tpy*, we observe and identify five different adsorption configurations, and we can show and rationalize their dependence on deposition and annealing temperature, a very important variable in practical situations of heterogeneous catalysis. The five observed configurations are explained in terms of intact physisorption, intact chemisorption, H-dissociated chemisorption, and combinations thereof. They illustrate the richness of adsorption modes and consequential reaction pathways that can be expected in catalytic reactions under practical conditions.

Acknowledgements

This work was supported in part by Hong Kong RGC grant HKUST 602008, Hong Kong RGC Grant CityU 102408, and the CityU Centre for Applied Computing and Interactive Media.

References

- [1] C. Díaz, E. Pijper, R.A. Olsen, H.F. Busnengo, D.J. Auerbach, G.J. Kroes, *Science* 326 (2009) 832.
- [2] K. Honkala, A. Hellman, I.N. Remediakis, A. Logadottir, A. Carlsson, S. Dahl, C.H. Christensen, J.K. Nørskov, *Science* 307 (2005) 555.
- [3] G.A. Somorjai, Y. Li, *Introduction to Surface Chemistry and Catalysis*, 2nd ed., Wiley, 2010.
- [4] K.W. Kolasinski, *Surface Science: Foundations of Catalysis and Nanoscience*, Wiley, 2008.
- [5] T. Katayama, K. Mukai, S. Yoshimoto, J. Yoshinobu, *J. Phys. Chem. Lett.* 1 (2010) 2917.
- [6] X. Shi, R.Q. Zhang, C. Minot, K. Hermann, M.A. Van Hove, W. Wang, N. Lin, *J. Phys. Chem. Lett.* 1 (2010) 2974.
- [7] P.S. Bagus, K. Hermann, C. Wöll, *J. Chem. Phys.* 123 (2005) 184109.
- [8] M.-T. Nguyen, C.A. Pignedoli, M. Treier, R. Fasel, D. Passerone, *Phys. Chem. Chem. Phys.* 12 (2010) 992.
- [9] G. Kresse, D. Joubert, *Phys. Rev. B* 59 (1999) 1758.
- [10] P.E. Blöchl, *Phys. Rev. B* 50 (1994) 17953.
- [11] J.J. Mortensen, L.B. Hansen, K.W. Jacobsen, *Phys. Rev. B* 71 (2005) 035109.
- [12] G. Kresse, J. Furthmüller, *Comput. Mater. Sci.* 6 (1996) 15.
- [13] G. Román-Pérez, J.M. Soler, *Phys. Rev. Lett.* 103 (2009) 096102.
- [14] M. Dion, H. Rydberg, E. Schröder, D.C. Langreth, B.I. Lundqvist, *Phys. Rev. Lett.* 92 (2004) 246401.
- [15] W. Wang, S. Wang, X. Li, J.-P. Collin, J. Liu, P.N. Liu, N. Lin, *J. Am. Chem. Soc.* 132 (2010) 8774.
- [16] S.J. Blanksby, G.B. Ellison, *Acc. Chem. Res.* 36 (2003) 255.